

Technical Report ARWSB-TR-12003

INFLUENCE AND MODELING OF RESIDUAL STRESSES IN THICK WALLED PRESSURE VESSELS WITH THROUGH HOLES

E. Troiano, A.P. Parker, and J.H. Izzo

February 2012



ARMAMENT RESEARCH, DEVELOPMENT AND ENGINEERING CENTER
Weapons & Software Engineering Center
Benét Laboratories



Approved for public release; distribution is unlimited (February 2012).

The views, opinions, and/or findings contained in this report are those of the author(s) and should not be construed as an official Department of the Army position, policy, or decision, unless so designated by other documentation.

The citation in this report of the names of commercial firms or commercially available products or services does not constitute official endorsement by or approval of the U.S. Government.

Destroy this report when no longer needed by any method that will prevent disclosure of its contents or reconstruction of the document. Do not return to the originator.

REPORT DOCUMENTATION PAGEForm Approved
OMB No. 0704-0188

Public reporting burden for this collection of information is estimated to average 1 hour per response, including the time for reviewing instructions, searching data sources, gathering and maintaining the data needed, and completing and reviewing the collection of information. Send comments regarding this burden estimate or any other aspect of this collection of information, including suggestions for reducing this burden to Washington Headquarters Service, Directorate for Information Operations and Reports, 1215 Jefferson Davis Highway, Suite 1204, Arlington, VA 22202-4302, and to the Office of Management and Budget, Paperwork Reduction Project (0704-0188) Washington, DC 20503.

PLEASE DO NOT RETURN YOUR FORM TO THE ABOVE ADDRESS.

1. REPORT DATE (DD-MM-YYYY) 28/02/2012		2. REPORT TYPE Technical Report		3. DATES COVERED (From - To)	
4. TITLE AND SUBTITLE Influence and Modeling of Residual Stresses in Thick Walled Pressure Vessels with Through Holes				5a. CONTRACT NUMBER	
				5b. GRANT NUMBER	
				5c. PROGRAM ELEMENT NUMBER	
6. AUTHOR(S) E. Troiano, A.P. Parker, and J. H. Izzo				5d. PROJECT NUMBER	
				5e. TASK NUMBER	
				5f. WORK UNIT NUMBER	
7. PERFORMING ORGANIZATION NAME(S) AND ADDRESS(ES) U.S. Army ARDEC Benet Laboratories, RDAR-WSB Watervliet, NY 12189-4000				8. PERFORMING ORGANIZATION REPORT NUMBER ARWSB-TR-12003	
9. SPONSORING/MONITORING AGENCY NAME(S) AND ADDRESS(ES) U.S. Army ARDEC Benet Laboratories, RDAR-WSB Watervliet, NY 12189-4000				10. SPONSOR/MONITOR'S ACRONYM(S)	
				11. SPONSORING/MONITORING AGENCY REPORT NUMBER	
12. DISTRIBUTION AVAILABILITY STATEMENT Approved for public release; distribution is unlimited (February 2012).					
13. SUPPLEMENTARY NOTES To be published in the Journal of Pressure Vessel Technology. To be presented at the 2012 ASME Pressure Vessel and Piping Division Conference - July 15-19, 2012 in Toronto, Ontario, Canada.					
14. ABSTRACT This study utilizes the classic stress based Paris Law fatigue life approach which takes into account the residual stresses as a function of radial location to assess the life of the vessel in the region of both configurations of through holes. It quantifies the concentration of stresses associated with the perpendicular and angled evacuator holes, and the amount of pressure that actually enters the evacuator hole. The analysis is employed to ensure that the life within these through holes meets or exceeds the safe life of the vessel without evacuator holes which has been determined by the 90% lower confidence bound on the 0.1th percentile on the population from the results of a minimum of six tests.					
15. SUBJECT TERMS Bauschinger Effect; evacuator hole; autofrettage; residual stress; thick walled cylinders; pressure vessels; and Paris Law					
16. SECURITY CLASSIFICATION OF:			17. LIMITATION OF ABSTRACT U/U	18. NUMBER OF PAGES 20	19a. NAME OF RESPONSIBLE PERSON Edward Troiano
a. REPORT U/U	b. ABSTRACT U/U	c. THIS PAGE U/U			19b. TELEPHONE NUMBER (Include area code) 518-266-5112

INSTRUCTIONS FOR COMPLETING SF 298

1. REPORT DATE. Full publication date, including day, month, if available. Must cite at least the year and be Year 2000 compliant, e.g., 30-06-1998; xx-08-1998; xx-xx-1998.

2. REPORT TYPE. State the type of report, such as final, technical, interim, memorandum, master's thesis, progress, quarterly, research, special, group study, etc.

3. DATES COVERED. Indicate the time during which the work was performed and the report was written, e.g., Jun 1997 - Jun 1998; 1-10 Jun 1996; May - Nov 1998; Nov 1998.

4. TITLE. Enter title and subtitle with volume number and part number, if applicable. On classified documents, enter the title classification in parentheses.

5a. CONTRACT NUMBER. Enter all contract numbers as they appear in the report, e.g. F33615-86-C-5169.

5b. GRANT NUMBER. Enter all grant numbers as they appear in the report, e.g. 1F665702D1257.

5c. PROGRAM ELEMENT NUMBER. Enter all program element numbers as they appear in the report, e.g. AFOSR-82-1234.

5d. PROJECT NUMBER. Enter all project numbers as they appear in the report, e.g. 1F665702D1257; ILIR.

5e. TASK NUMBER. Enter all task numbers as they appear in the report, e.g. 05; RF0330201; T4112.

5f. WORK UNIT NUMBER. Enter all work unit numbers as they appear in the report, e.g. 001; AFAPL30480105.

6. AUTHOR(S). Enter name(s) of person(s) responsible for writing the report, performing the research, or credited with the content of the report. The form of entry is the last name, first name, middle initial, and additional qualifiers separated by commas, e.g. Smith, Richard, Jr.

7. PERFORMING ORGANIZATION NAME(S) AND ADDRESS(ES). Self-explanatory.

8. PERFORMING ORGANIZATION REPORT NUMBER. Enter all unique alphanumeric report numbers assigned by the performing organization, e.g. BRL-1234; AFWL-TR-85-4017-Vol-21-PT-2.

9. SPONSORING/MONITORS AGENCY NAME(S) AND ADDRESS(ES). Enter the name and address of the organization(s) financially responsible for and monitoring the work.

10. SPONSOR/MONITOR'S ACRONYM(S). Enter, if available, e.g. BRL, ARDEC, NADC.

11. SPONSOR/MONITOR'S REPORT NUMBER(S). Enter report number as assigned by the sponsoring/ monitoring agency, if available, e.g. BRL-TR-829; -215.

12. DISTRIBUTION/AVAILABILITY STATEMENT. Use agency-mandated availability statements to indicate the public availability or distribution limitations of the report. If additional limitations/restrictions or special markings are indicated, follow agency authorization procedures, e.g. RD/FRD, PROPIN, ITAR, etc. Include copyright information.

13. SUPPLEMENTARY NOTES. Enter information not included elsewhere such as: prepared in cooperation with; translation of; report supersedes; old edition number, etc.

14. ABSTRACT. A brief (approximately 200 words) factual summary of the most significant information.

15. SUBJECT TERMS. Key words or phrases identifying major concepts in the report.

16. SECURITY CLASSIFICATION. Enter security classification in accordance with security classification regulations, e.g. U, C, S, etc. If this form contains classified information, stamp classification level on the top and bottom of this page.

17. LIMITATION OF ABSTRACT. This block must be completed to assign a distribution limitation to the abstract. Enter UU (Unclassified Unlimited) or SAR (Same as Report). An entry in this block is necessary if the abstract is to be limited.

ABSTRACT

Thick walled pressure vessels are often autofrettaged in order to impart favorable near bore compressive residual stresses which can significantly increase the life of the vessels. These stresses can be imparted via a thermal shrink process in which there is no loss of residual stresses due to the Bauschinger Effect, or more economically with a mechanical swage or hydraulic overload process in which the Bauschinger Effect is present.

In some cases these vessels have holes bored through the wall in order to take advantage of the escaping gasses for actuation of external peripherals associated with the vessel. These through holes which can be angled or perpendicular to the centerline of the major axis of the pressure vessel can significantly reduce the life of the vessel depending on the wall ratio of the vessel as well as the, angle of inclination of the hole to the centerline of the vessel.

This study utilizes the classic stress based Paris Law fatigue life approach which takes into account the residual stresses as a function of radial location to assess the life of the vessel in the region of both configurations of through holes. It quantifies the concentration of stresses associated with the perpendicular and angled evacuator holes, and the amount of pressure that actually enters the evacuator hole. The analysis is employed to ensure that the life within these through holes meets or exceeds the safe life of the vessel without evacuator holes which has been determined by the 90% lower confidence bound on the 0.1th percentile on the population from the results of a minimum of six tests.

Table of Contents

ABSTRACT.....	i
NOMENCLATURE	1
INTRODUCTION	1
STRESS CONCENTRATION EFFECTS OF A THOUGH HOLE IN A PRESSURISED VESSEL.....	3
STRESSES IN THICK WALLED CYLINERS.....	5
LAME STRESSES.....	5
RESIDUAL AUTOFRETTAGE STRESSES	5
EVACUATOR PRESSURE STRESSES.....	7
FATIGUE LIFE ANALYSIS	7
COMPARISON OF MEASURED LIVES	7
PREDICTION OF FUTURE EVACUATOR HOLE LIVES	8
ASSESSMENT OF INITIAL DAMAGE	8
ASSESSMENT OF STRESSES	10
LABORATORY LIFE ASSESSMENT	11
FIELD SERVICE LIFE ASSESSMENT.....	12
CONCLUSIONS.....	13
REFERENCES	14

List of Tables

TABLE 1	K_t FOR VARIOUS A, B, c AND r_2/r_1	4
TABLE 2	INPUTS USED IN LIFE ANALYSIS	8
TABLE 3	LIFE COMPARSION WITH PREVIOUSLY PUBLISHED REPORTS	8
TABLE 4	LABORATORY LIFE COMPARISON OF EVACUATOR HOLES	12

LIST OF ILLUSTRATIONS

FIGURE 1	NOMENCLATURE	1
FIGURE 2	STRESS CONCENTRATION EFFECTS IN BI-AXIAL STRESS FIELD.....	6
FIGURE 3	VIEW LOOKING IN THE R DIRECTION IN A STRAIGHT THROUGH EVACUATOR HOLE	9
FIGURE 4	ENVIRONMENTAL CRACKING OBSERVED IN EVACUATOR HOLE.....	9
FIGURE 5	STRESSES PRESENT IN STRAIGHT EVACUATOR HOLE (C=1.0), OPEN ENDED VESSEL, 100% OVERSTRAIN, WITH 20% OF PRESSURE ENTERING HOLE.....	10
FIGURE 6	STRESSES PRESENT IN ANGLED EVACUATOR HOLE (C=2.0), OPEN ENDED VESSEL, 100% OVERSTRAIN, WITH 20% OF PRESSURE ENTERING HOLE.....	10
FIGURE 7	CROSS SECTION OF ANGLED EVACUATOR HOLE SHOWING DEPTH OF SEAL AND LOCATION OF FATIGUE DAMAGE.....	11
FIGURE 8	LIFE AS A FUNCTION OF WALL LOCATIONS WITH 100% OF PRESSURE ENTERING THE EVACUATOR HOLES	13

NOMENCLATURE

a_i, a_f	initial, final crack length
α	angle to centerline of evacuator hole
p	internal pressure of vessel
r_1	inside radius
r_2	outside radius
r	radial wall location
σ_{YS}	Material Yield Strength
ρ	elastic/plastic interface
β	Bauschinger Effect Factor
K_t	Stress Concentration Factor
C	Paris Law Coefficient
n	Paris Law Exponent
$\Delta\sigma_{\text{effective}}$	effective stress range
A	fraction of pressure in through hole
c'	minor axis of through hole
d'	major axis of through hole
c	elliptical aspect ratio of through hole ($=d'/c'$)
f	crack shape factor
x	non dimensioned wall location
W	wall ratio
R, θ, z	radial, angular and axial orientation respectively with z coinciding with centerline of the major axis of cylinder

INTRODUCTION

Often times pressure vessels are manufactured with various through wall holes in order to take advantage of the pressure within the vessel and utilize it for working external components associated with the vessel. These through wall holes are often inclined to the major axis of the vessel at some angle α which is referenced from the centerline of the vessel. Typically the angle of inclination varies between 30° and 90° when measured from the major axis of the vessel. (Figure 1). Also defined in Figure 1 is d' or the major axis of the through hole and c' which is the minor axis of the through hole, as well as the aspect ratio, c , defined as d'/c' which is the ratio of the ellipse created as the through hole intersects the bore surface.

O'Hara [1] investigated stress concentration factors of through holes in vessels that are orientated in the R - θ plane and intersect the bore on a radial 45° tangent to the bore surface. This type of through hole results in an ellipse at the bore surface which is orientated so that the major axis of the resultant ellipse is perpendicular to that depicted in Figure 1. This orientation results in a decreased stress concentration factor due to the fact that the larger radius of curvature (associated with the c') is now orientated with the hoop stresses, which predominately control fatigue failure.

Although his analysis clearly showed a decrease in the stress concentration factor of a through hole which intersected the bore on a radial 45° tangent to the bore surface, his proposals have never been implemented.

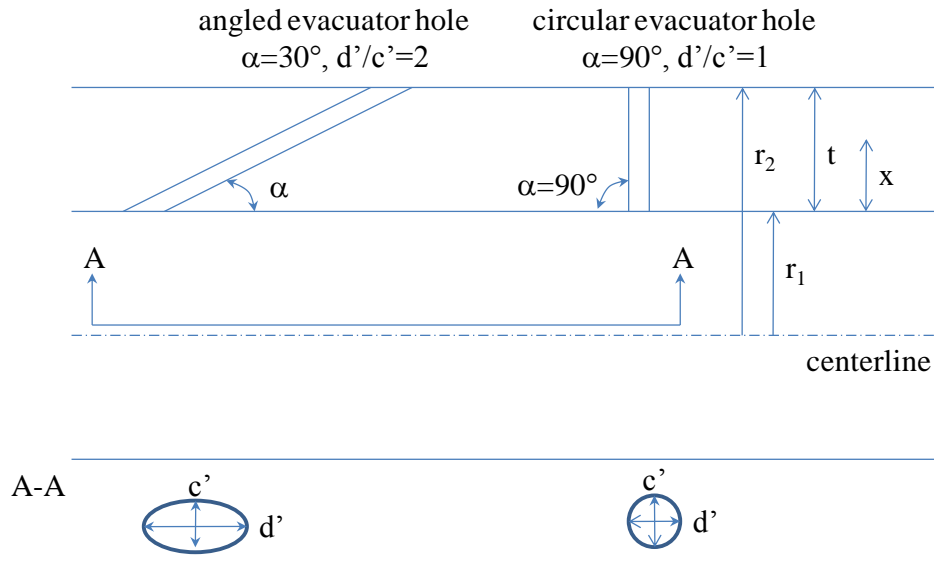


Figure 1: Nomenclature

Cheng [2] also investigated the effects of the stress concentration factor created by through holes and provided an equation for a pressurized open ended cylinder with a through hole in the R-z plane as is depicted in Figure 1. However, his photoelastic measurements consistently produced K_t lower than the analytical predictions.

Subsequent work by Nagamatsu et al [3] showed that when a vessel is rapidly pressurized with gas only a small fraction of the vessel's pressure enters the evacuator hole because of the choking nature of gasses when exiting the vessel and entering the evacuator hole. Nagamatsu's results clearly showed that only about 20% of the bore pressure enters these small (d' and $c' \ll r_1$) evacuator holes.

Additional studies by Underwood et al [4] looked into the effects of partial pressure entering the evacuator hole and concluded that the fatigue limiting initiation position along the length of the evacuator hole is driven by the location of the elastic/plastic boundary imparted during the autofrettage process. Underwood's analysis was simplified by overlooking the correct full wall autofrettage residual stress fields as well as assuming that the final crack length a_f , was the full wall thickness of the pressure vessel and independent of the actual radial wall location in the evacuator hole where the cracking was initiated. Typically the final crack length has little influence on the lives predicted; however if the crack initiation site is near the outside diameter of the vessel and the initial crack depth a_i is of a similar magnitude to a_f , the remaining ligament can have a dramatic effect on the predicted remaining life. This analysis will address these issue and others.

STRESS CONCENTRATION EFFECTS OF A THROUGH HOLE IN A PRESSURISED VESSEL

The stress concentration factor, K_t for a through wall hole in a pressurized cylinder is a function of the inner and outer radius of the pressure vessel, the aspect ratio, c of the through hole as well as the pressure that enters the evacuator hole.

Little & Bagci [5,6] examined stress concentration effects for small through holes in a pressurized thick walled cylinder. For the closed-end case the stress concentration factor as given by Cheng in reference 2 is:

$$K_t = (4cr_2^2 + r_1^2) / (r_2^2 + r_1^2) \quad (1)$$

and for the open-end case is given by:

$$K_t = (4cr_2^2 + 2r_1^2) / (r_2^2 + r_1^2) \quad (2)$$

These solutions are valid for the bore of a pressurized thick walled cylinder intersected by a small elliptical hole where d' and $c' \ll r_1$. These holes are inclined in the R-z plane, with zero inclination in the R- θ plane, thereby producing an elliptical shape where they intersect the bore of the pressure vessel similar to the one depicted in Figure 1. These solutions are limited because they assume that the full bore pressure acts within the evacuator hole. However as previously noted, the creation of a shock wave at the evacuator hole-bore intersection results in a choking effect, with only a proportion of bore pressure getting into the evacuator hole.

In order to determine K_t for a range of pressures within the evacuator hole, Cheng's equations were reformulated for the case in which a proportion A ($0 \leq A \leq 1$) of the bore pressure acts within the evacuator hole.

To further generalize the expression for K_t the axial stress σ_z is defined in terms of B , where:

$$B = (\sigma_z/p) [(r_2^2/r_1^2) - 1] \quad (3)$$

Where the specific end-conditions include [7]

$B = 0$ for the open-end case

$B = 1$ for the closed-end case

$B = 2 \times$ Poisson's Ratio for zero axial strain

With these additions, following the analysis sequence in [5] and [6], the single general expression for K_t can be written as:

$$K_t = \{ r_2^2 [(2c+1) + A(2c-1)] + r_1^2 [(2c+1-B) - A(2c-1)] \} / (r_2^2 + r_1^2) \quad (4)$$

Equation (4) reduces to Cheng's solution, eqn (1) above, for $A = 1$, $B = 1$ (full pressure in evacuator, closed ends) and Cheng's solution, eqn (2) for $A = 1$, $B = 0$ (full pressure in evacuator, open ends)

Equation (4) further reduces to:

$$K_t = [r_2^2(2c+1) + r_1^2(2c)]/(r_2^2+r_1^2) \quad (5)$$

for $A = 0$, $B = 1$ (no pressure in evacuator, closed ends)

Table 1 displays the specific K_t for various A , B , c and r_2/r_1 .

End condition B	% pressure in hole A	r_2/r_1	c	K_t
closed (B=1)	100 (A=1)	2	2	6.60
closed (B=1)	0 (A=0)	2	2	4.80
closed (B=1)	0 (A=0.2)	2	2	5.16
open (B=0)	100 (A=1)	2	2	6.80
open (B=0)	0 (A=0)	2	2	5.00
open (B=0)	20 (A=0.2)	2	2	5.36
closed (B=1)	100 (A=1)	2	1	3.40
closed (B=1)	0 (A=0)	2	1	2.80
closed (B=1)	0 (A=0.2)	2	1	2.92
open (B=0)	100 (A=1)	2	1	3.60
open (B=0)	0 (A=0)	2	1	3.00
open (B=0)	20 (A=0.2)	2	1	3.12
closed (B=1)	100 (A=1)	1.5	2	5.85
closed (B=1)	0 (A=0)	1.5	2	4.69
closed (B=1)	0 (A=0.2)	1.5	2	4.92
open (B=0)	100 (A=1)	1.5	2	6.15
open (B=0)	0 (A=0)	1.5	2	5.00
open (B=0)	20 (A=0.2)	1.5	2	5.23
closed (B=1)	100 (A=1)	1.5	1	3.08
closed (B=1)	0 (A=0)	1.5	1	2.69
closed (B=1)	0 (A=0.2)	1.5	1	2.77
open (B=0)	100 (A=1)	1.5	1	3.38
open (B=0)	0 (A=0)	1.5	1	3.00
open (B=0)	20 (A=0.2)	1.5	1	3.08

Table 1: K_t for various A , B , c and r_2/r_1

STRESSES IN THICK WALLED CYLINERS

Since these vessels are 100% overstrained, the effective stresses in them are the combinations of several stresses acting together that control the life of the vessel. Those stresses include the Lamé or pressure loading stresses, the autofrettage residual stresses and the stresses acting within the hole as a result of the pressure that enters the evacuator hole. Since the hoop stresses are the controlling stresses they are the ones that will be concentrated on in this discussion. The general equation that represents these effective stresses can be written as

$$\sigma_{\text{effective}} = K_t * \sigma_{\text{Lame}} + K_t * \sigma_{\text{residual}} + \sigma_{\text{pressure}} \quad (6)$$

These stresses and their associated governing equation are presented next.

LAME STRESSES

The Lamé stresses are the stresses which result from the pressure loading of the vessel. The most important of the Lamé stresses are the hoop stresses since they control the fatigue life of the vessel. The equation for the Lamé hoop stresses [8] can be written as

$$\sigma_{\text{Lame}} = [-\rho r_1^2 / (r_2^2 - r_1^2)] (1 + r_2^2 / r^2) - A_p \quad (7)$$

Where the A_p term accounts for the fraction of pressure acting on the surface of the crack in the evacuator hole. If σ_{Lame} times the appropriate K_t exceeds the material yield strength σ_{YS} we simply cap the σ_{Lame} at the materials yield strength. Although capping of the Lamé stress at the yield strength allows us to simplify the analysis, there is some error introduced by neglecting cyclic plasticity effects including cyclic strain hardening.

RESIDUAL AUTOFRETTAGE STRESSES

The hoop autofrettage residual stresses are induced as a result of the plastic straining during the autofrettage process and can be written as [9]

$$\sigma_{\text{auto-hoop-plastic}} = \sigma_{\text{YS}} \left[\left(\frac{r_1^2}{r_2^2 - r_1^2} \right) \left(1 + \frac{r_2^2}{r^2} \right) \left(\frac{\rho^2 - r_2^2}{2r_2^2} - \text{LN}(\rho/r_1) \right) + \left(\frac{\rho^2 + r_2^2}{2r_2^2} - \text{LN}(\rho/r) \right) \right] \quad (8)$$

for $r_1 < r < \rho$

and

$$\sigma_{\text{auto-hoop-elastic}} = \sigma_{\text{YS}} \left(1 + \frac{r_2^2}{r^2} \right) \left[\left(\frac{\rho^2}{2r_2^2} + \left(\frac{r_1^2}{r_2^2 - r_1^2} \right) \left(\frac{\rho^2 - r_2^2}{2r_2^2} - \text{LN}(\rho/r_1) \right) \right) \right] \quad (9)$$

for $\rho < r < r_2$

where

$$\rho = (r_2 - r_1) * \% \text{ autofrettage} + r_1 \quad (10)$$

However this is not the only stress from autofrettage acting in the hoop direction. The autofrettage process also induces a residual axial stress field. This stress field along with the typical hoop stress field is shown schematically in Figure 2, along with the results superimposed to give the total residual stress field in the vicinity of the hole.

We have assumed for this analysis that the axial stress is 1/3 of the hoop stress with the same sign as the hoop stresses. This simplification will be used in this analysis, however past work by Davidson et al [10] and more recently work by O'Hara [11] suggests that this simplification may be in error. Their findings have suggested that in swaged tubes the axial stresses vary in magnitude and sign depending on the percentage of autofrettage as well as the wall ratio, W , of the vessel.

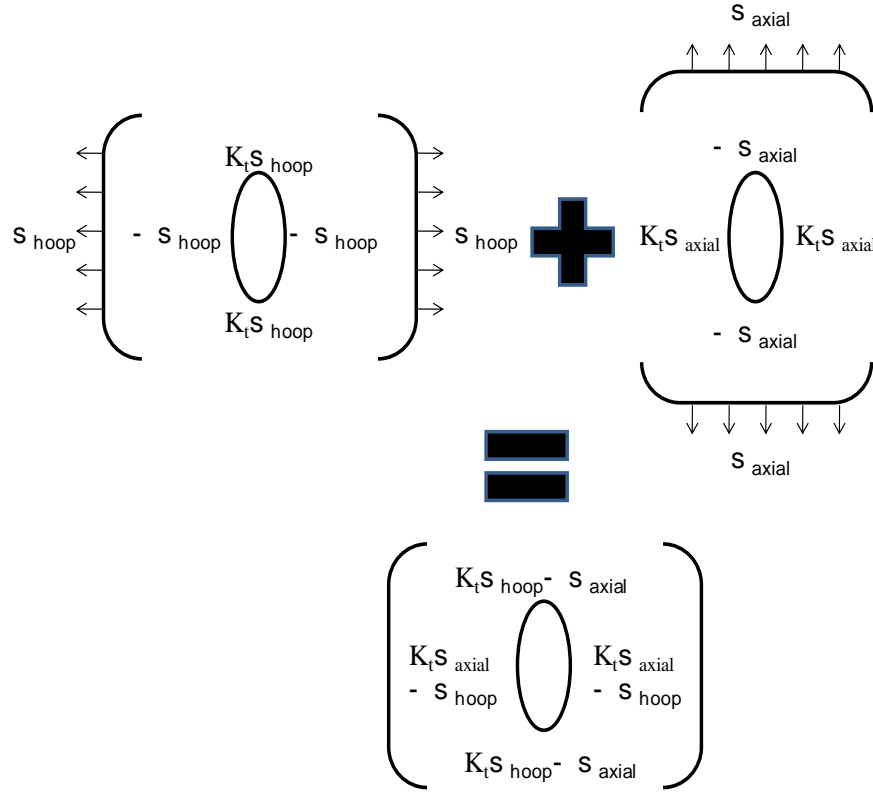


Figure 2: Stress concentration effects in bi-axial stress field.

If $K_t * \sigma_{auto-hoop-plastic} - \sigma_{Axial}$ exceeds $-\sigma_{YS}$ then we must account for the loss of reverse loading strength also known as the Bauschinger Effect Factor, β . For this analysis the β was assumed to be a constant with $\beta = 0.7$. Under this condition the residual stress to utilize in equation 7 becomes

$$\sigma_{residual} = \beta * (K_t \sigma_{auto-hoop-plastic} - \sigma_{Axial}) \quad (11)$$

Whereas if the $\sigma_{auto-hoop-elastic}$ times the appropriate K_t exceeds σ_{YS} we simply cap the $\sigma_{auto-hoop-elastic}$ at the materials yield strength. As in the case of the Lamé stress, capping of the residual stress at the yield stress allows us to simplify the analysis and may lead to some error.

EVACUATOR PRESSURE STRESSES

Since the results published in [3] suggest that only a fraction of the bore pressure enters the evacuator hole, we need to account the stresses in the hole as a result of the pressure as

$$\sigma_{\text{pressure}} = -Ap \quad (14)$$

Once each of the stresses in Equation 6 are calculated and summed, if the effective stress is in excess of the material yield strength the effective stress is capped at the materials yield strength, which again may lead to some error in the analysis.

FATIGUE LIFE ANALYSIS

Fatigue life analysis utilizes the well know Paris Law

$$da/dN = C \Delta K^n \quad (15)$$

where the effective stress intensity range is approximated as

$$\Delta K = 1.12f \Delta\sigma_{\text{effective}} \sqrt{\pi a} \quad (16)$$

and $\Delta\sigma_{\text{eff}}$ represents the positive portion of the summation of stresses from equation 6 including the effect of the residual stress, which is not an alternating stress but a constant stress. This assumption allows us to simplify the analysis by neglecting any R-ratio effects and it results in a conservative lower bound prediction on life. We have also defined the crack shape factor $f = 0.75$ for an elliptically shaped crack. Once equation 15 is integrated it takes the form for predicting life as

$$N = 2[1/\sqrt{a_i} - 1/\sqrt{a_f}] / C (1.12f \Delta\sigma_{\text{effective}} \sqrt{\pi})^n \quad (17)$$

The Paris Law coefficients C and n were measured for the ASTM A723 low alloy, high strength steels by following ASTM E647 test standard and found to be $C = 1.43E-11$ and $n = 2.67$ in SI units.

COMPARISON OF MEASURED LIVES

Underwood [4] provided a comparison of his analysis of evacuator holes with actual test data. As a check we utilized his inputs with the methodology previously presented to test the validity of this method and to see if the added fidelity of this model made for a more accurate prediction of lives. The inputs to the comparison analysis are presented in Table 2 along with the all important initial flaw size that was assumed to be $10\mu\text{m}$ [12]. The resultant comparisons lives along with statistical analysis of the results are presented in the Table 3.

Vessel #	σ_{YS} MPa	r_1 mm	r_2 mm	Overstrain %	p MPa
35A	1260	53	76	0	207
35B	1210	53	76	0	207
86A	1250	53	81	100	207
25A	1090	60	94	29	297
25B	1090	60	94	29	297
91A	1190	60	94	49	297
91B	1140	60	94	49	297
85A	1220	78	107	100	83
85B	1220	78	107	100	83

Table 2: Inputs used in life analysis

The $N_{0.2P}$ represents the result using the method in this report assuming that 20% of the pressure enters the evacuator hole. The $N_{measured}$ and the $N_{0.2P}^4$ represent the actual measured lives and the predictions made in reference [4] respectively. Note the statistical mean and standard deviation of this analysis compare favorably with the actual test data, and suggest that this method is a better predictor of life than that presented in [4].

Vessel #	x/t	$N_{measured}$ (cycles)	$N_{0.2P}$ (cycles)	$N_{0.2P}^4$ (cycles)
35A	0.00	4710	6984	6970
35B	0.00	5770	7886	6970
86A	0.47	9780	8189	24060
25A	0.24	4780	12116	6860
25B	0.24	3540	12116	6860
91A	0.36	3520	8769	8400
91B	0.36	3550	9907	8400
85A	0.48	43340	47311	139200
85B	0.48	40710	47311	139200
Mean		13300	17843	38547
St Dev		16413	16800	57328

Table 3: Life comparison with previously published reports

PREDICTION OF FUTURE EVACUATOR HOLE LIVES

ASSESSMENT OF INITIAL DAMAGE

Through investigation was undertaken on vessels similar in size and strength level to pressure vessels 85A and 85B however the internal pressure was increased from 83MPa to 124MPa. Microstructural investigation as to the damage in these vessels in the evacuator holes, which was the resultant of thousands of service cycles, revealed defects ranging up to 1000 μ m in both the angled evacuator holes and the straight evacuator holes. These flaws appeared to be a combination of general corrosion pitting damage shown in Figure 3, and inter-granular branched

cracking damage shown in Figure 4. In both Figure 3 and Figure 4 the centerline of the pressure vessel is from left to right.

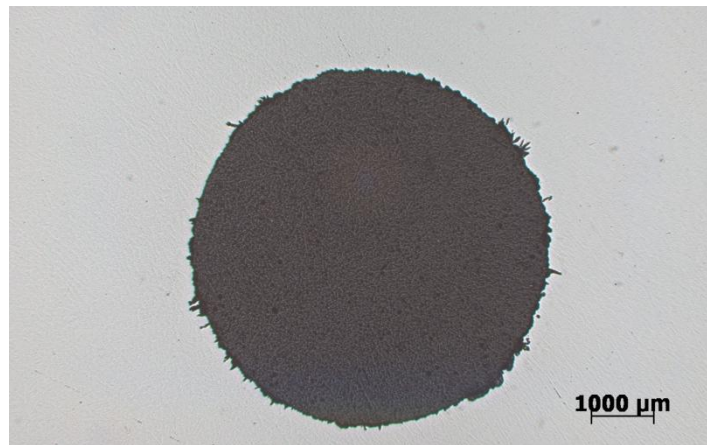


Figure 3: View looking in the R direction in a straight through evacuator hole.

One interesting feature to note is that the inter-granular cracking in the evacuator holes appears to be randomly distributed along both the length of the evacuator hole as well as around the circumference of the evacuator hole, suggesting that the source of the residual stresses required to initiate and propagate these environmental cracks is not a resultant of the typical autofrettage residual stresses, which would cause these cracks to be patterned in a predictable manner. The random nature of these cracks indicates a random residual stress state which is speculated to be induced during the manufacturing process in some as of yet unknown fashion. These environmental cracks act as initiation sites for subsequent crack extension from mechanical loading. Also of significant importance here is that this is the first time we have ever observed environmental cracking from field service that is not accompanied by thermal damage.

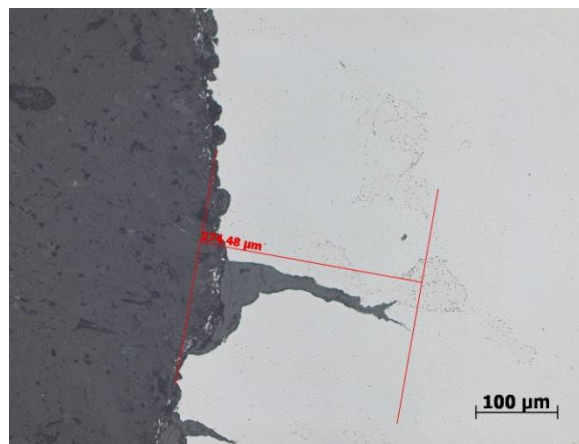


Figure 4: Environmental cracking observed in evacuator hole.

ASSESSMENT OF STRESSES

The resultant of the analysis of the stresses following the methodology previously presented is shown in Figure 5 for a straight through evacuator hole in an open ended pressure vessel with $W=1.37$, bore pressure of 124MPa, 20% of the pressure entering the evacuator hole and 100% autofrettage.

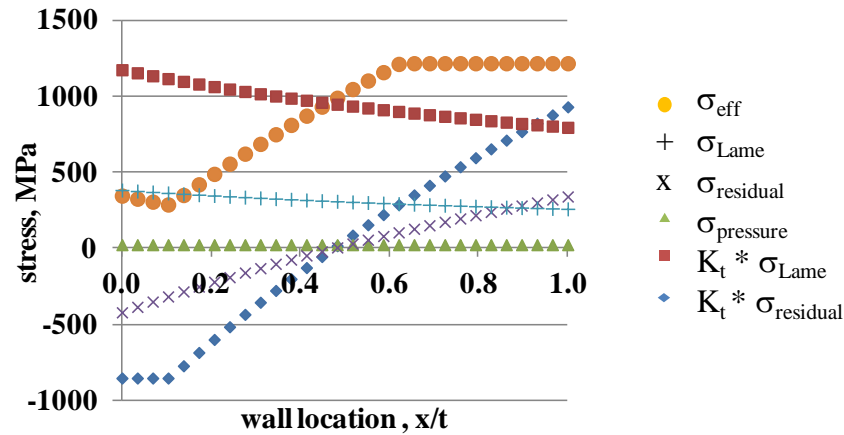


Figure 5: Stresses present in straight evacuator hole ($c=1.0$), open ended vessel, 100% overstrain, with 20% of pressure entering hole.

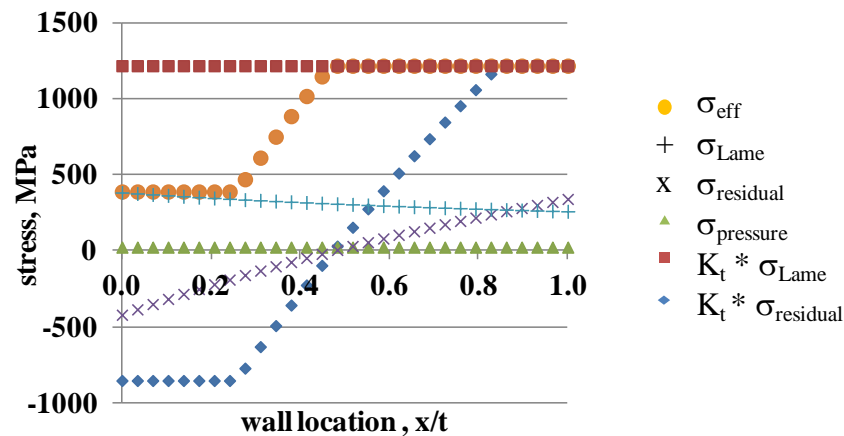


Figure 6: Stresses present in angled evacuator hole ($c=2.0$), open ended vessel, 100% overstrain with 20% of pressure entering hole.

Figure 6 represents the stresses in an angled evacuator hole, $\alpha=30^\circ$, open ended pressure vessel with $W=1.37$, bore pressure of 124MPa, 20% of the pressure entering the evacuator hole and 100% autofrettaged. Observe from the plots the stress resulting from the pressure in the evacuator hole, $\sigma_{pressure}$. These stresses are shown to be the smallest stress in magnitude of all the stresses, and hence they play the least significant role in estimating lives. However, his stress poses a difficulty when trying to reproduce them it in a laboratory setting since the same hydraulic pressure used to pressurize the bore of the vessel is used to pressurize the evacuator

hole and there is no choking effect similar to service loading. Hence the decision was made during laboratory testing to test the evacuator hole at full bore pressure, which results in no change in $\Delta\sigma_{\text{effective}}$ in the highest stressed region from $x/t > 0.6$ for the straight hole and $x/t > 0.4$ for the angled hole since at these locations the $\Delta\sigma_{\text{effective}}$ was already greater than the material yield strength. Also adding to the complexity of the test is sealing issues in the evacuator holes. Typical wedge and o-ring seals were utilized, however in order to implement this type of seal, machining of the evacuator holes from the outside diameter of the pressure vessel is necessary. This machining process resulted in the removal of the critically stressed region near the outside diameter of the pressure vessel as can be seen in Figure 7 for the angled evacuator hole. In the case of the angled hole, the region between $x/t = 0.60$ to x/t of 1.0 was removed and in the case of the straight through hole the region between $x/t = 0.53$ to $x/t = 1.0$ was removed to allow for the seal seat.

LABORATORY LIFE ASSESMENT

Utilizing the effective stresses presented in Figure 5 and Figure 6, the average $a_{i\text{-measured}}$ from the inspection of each of the failure surfaces (which is shown in Table 4) and the previously presented C and n coefficients we can predict the life of the evacuator holes as a function of wall location from Equation 17. The predictions for the straight evacuator hole and angled evacuator hole along with the actual measured lives assuming full pressure in the evacuator holes, is shown in Table 4 and graphically in Figure 8. Note the lives predicted in the angled evacuator hole are essentially constant for $x/t > 0.4$. This is different than the lives predictions in [4] and is due to the fact these lives assume a decreasing a_f as x/t increases in equation 17. Whereas in reference [4] they assumed a constant a_f for all x/t . Also shown in Figure 8 is the wall location of the seals used to restrain the pressure. In the case of the angled hole it is shown as the short dotted line at $x/t = 0.6$ and for the straight hole it is shown as the long dotted at $x/t = 0.53$. The actual lives measured for these tests are shown as the triangles and squares in Figure 8 and are also presented in Table 4.



Figure 7: Cross section of angled evacuator hole showing depth of seal and location of fatigue damage.

Tube #	x/t	a _i -measured (μm)	orientation	N _{measured} (cycles)	N _{1.0P} (cycles)
85-1	0.57	730	angled	6146	7700
85-1	0.53	1000	straight	7191	11800
85-9	0.57	830	angled	5036	7100
85-9	0.53	900	straight	8356	13500
Mean		865			
SD		113.8			

Table 4: Laboratory life comparison of evacuator holes

FIELD SERVICE LIFE ASSESSMENT

Since the field service of these vessels is slightly different than laboratory simulated service we have extended the analysis to account for the lower evacuator pressure stresses as well as adding a safety factor based on a statistical analysis of the initial flaw sizes measured from the vessels in Table 4. The analysis follows similar logic to the prior analysis, except the A in equation 14 was reduced to 0.2. The factor of safety includes assessing the standard deviation (SD) of the initiation damage observed in the vessels in question, and then assuming 3 SD to account for the largest conceivable flaw with a 99.7% probability that the size of the flaw will be less than this flaw size. This equates to a flaw that is 1200 μm . The results of utilizing these inputs into equation 17 as a function of wall location results can be observed for the straight through hole and the angled hole in Figure 9. Also shown in Figure 9 is the statistical results from six full scale tests which estimated the operational life of these vessels as determined by the 90% lower confidence bound on the 0.1th percentile on the population from the results of a six tests, which equated to a life of 2600 cycles and is shown as the dashed line in Figure 9. Note the pressure in the evacuator hole has decreased however the lower predicted life in the holes is mainly the result of the application of the 3SD initial flaw size. In both Figure 8 and Figure 9 we have neglected the analysis after $x/t > 0.8$ since in this region other geometric features limit the accuracy of this type of analysis.

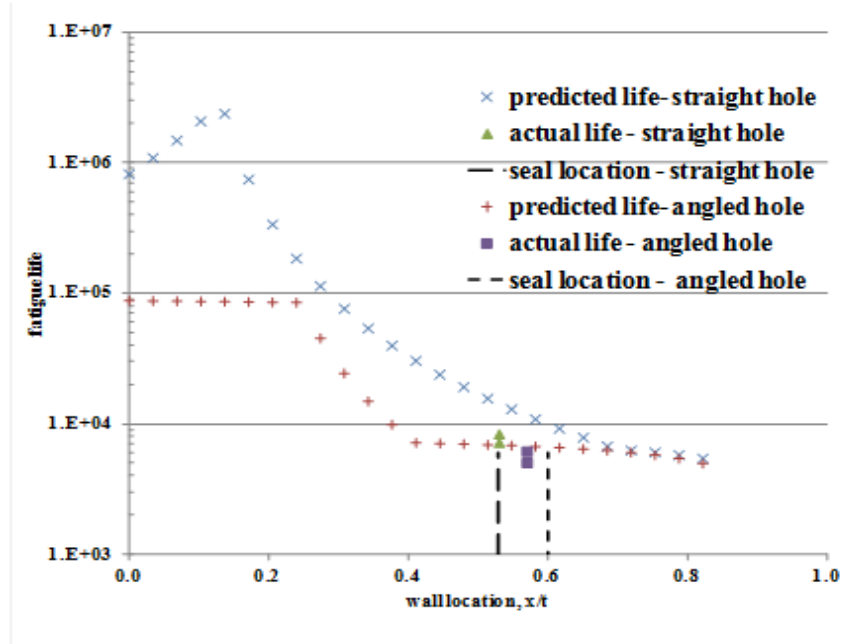


Figure 8: Life as a function of wall locations with 100% of pressure entering the evacuator holes.

CONCLUSIONS

1. Classical stress analysis and the use of the Paris Law have been utilized successfully to accurately predict lives in section with high magnitude localized plasticity by limiting maximum applied stresses at the materials yield point and minimum applied stresses to the product of the Bauschinger Effect Factor and the material yield strength.
2. A simple closed form solution has been evaluated for the stress concentration factor of a hole through the wall of a pressurized vessel.
3. Autofrettage play an important role in increasing the predictions of near bore fatigue life in angled evacuator holes but has no impact on life in the angled evacuator holes as x/t increases. This is due to the fact that the as x/t of approximately 0.4 in vessels that are heavily autofrettaged the effective stress in this location is well above the yield stress of the material.
4. For the same initial flaw size the life in the angled evacuator holes will always be less than or equal to the life in the straight though holes.

REFERENCES

1. O'Hara, G.P., "Experimental Investigation of Stress Concentration Factors of Holes in Thick Walled Cylinders", Benet Laboratories Technical Report WVT-6807, June 1986.
2. Cheng, Y.F., "Stress Concentration Around Inclined Holes in Pressurized Thick Walled Cylinders", ARDEC Technical Report ARLCB-TR-78019, November 1978.
3. Nagamatsu, H.T., Choi, K.T., Duffey, R.E., Carafano, G.C., "An Experimental and Numerical Study of the Flow Through a Vent Hole in a Perforated Muzzle Break", ARDEC Technical Report ARCCB-TR-87016, Benet Weapons Laboratory, Watervliet, New York, June 1987.
4. Underwood, J.H., Parker, A.P., Corrigan, D.J., and Audino, M.J., "Fatigue Life Measurements and Analysis for Overstrained Tubes With Evacuator Holes", J. of Pressure Vessel Technology, Vol. 118, Issue 4, November 1996.
5. Little, R. E., 1965, "Stress Concentrations for Holes in Cylinders", Machine Design, Dec 1965, pp 133-135.
6. Little, R. E. and Bagci, C., 1965, "Stress Analyses of Pressurized Cylinders", Engineering Research Bulletin, Publication No. 145, Oklahoma State University.
7. Chakrabarty, J, 1987, "Theory of Plasticity", McGraw-Hill, Singapore.
8. Shigley, J.E. and Mitchell, L.D., "Mechanical Engineering Design", McGraw-Hill.
9. Prager, W, and Hodge, P.C., Theory of Perfectly Plastic Solids", J Wiley and Sons, New York 1951.
10. Davidson, T.E., Kendall, D.P., and Reiner, A.N., 1963, "Residual Stresses in Thick-Walled Cylinders Resulting from Mechanically Induced Overstrain", Experimental Mechanics, 3, pp. 253-262.
11. O'Hara, G.P., Personal Conversations.
12. Underwood, J.H. and Parker, A.P., "Fatigue Life Analysis and Tests for Thick-Wall Cylinders Including the Effects of Overstrain and Axial Grooves", Proceedings of the 1994 ASME Pressure Vessel and Piping Conference, PVP Vol. 280, American Society of Mechanical Engineers, New York, 1994, pp. 303-311.